Supporting Information (SI)

Structural studies of thyroid peroxidase show the monomer interacting with autoantibodies in thyroid autoimmune disease

Daniel E. Williams, Sarah N. Le, David E. Hoke, Peter G. Chandler, Monika Gora, Marlena Godlewska, J. Paul Banga and Ashley M. Buckle

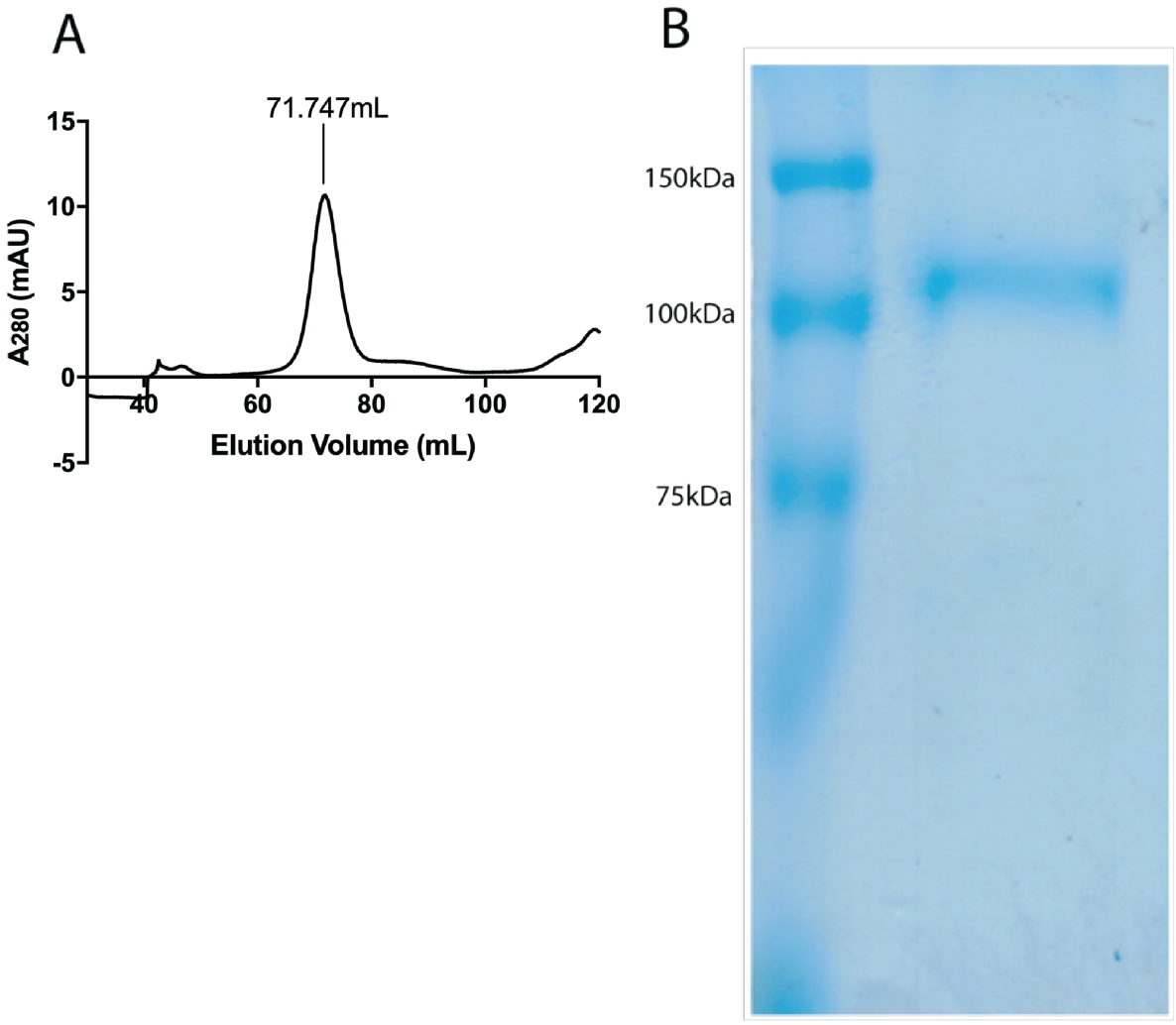

Figure S1 - Purification of the TPO construct ΔproTPOe-GCN4 (A) A chromatogram from a Superdex S200 16/60 column, showing ΔproTPOe-GCN4 eluting as a single major peak at 71.7mL, consistent with a 110 kDa protein. No other major large species appears to be present. **(B)** Reducing SDS-PAGE analysis of purified ΔproTPOe-GCN4 shows a major band at ~110 kDa.

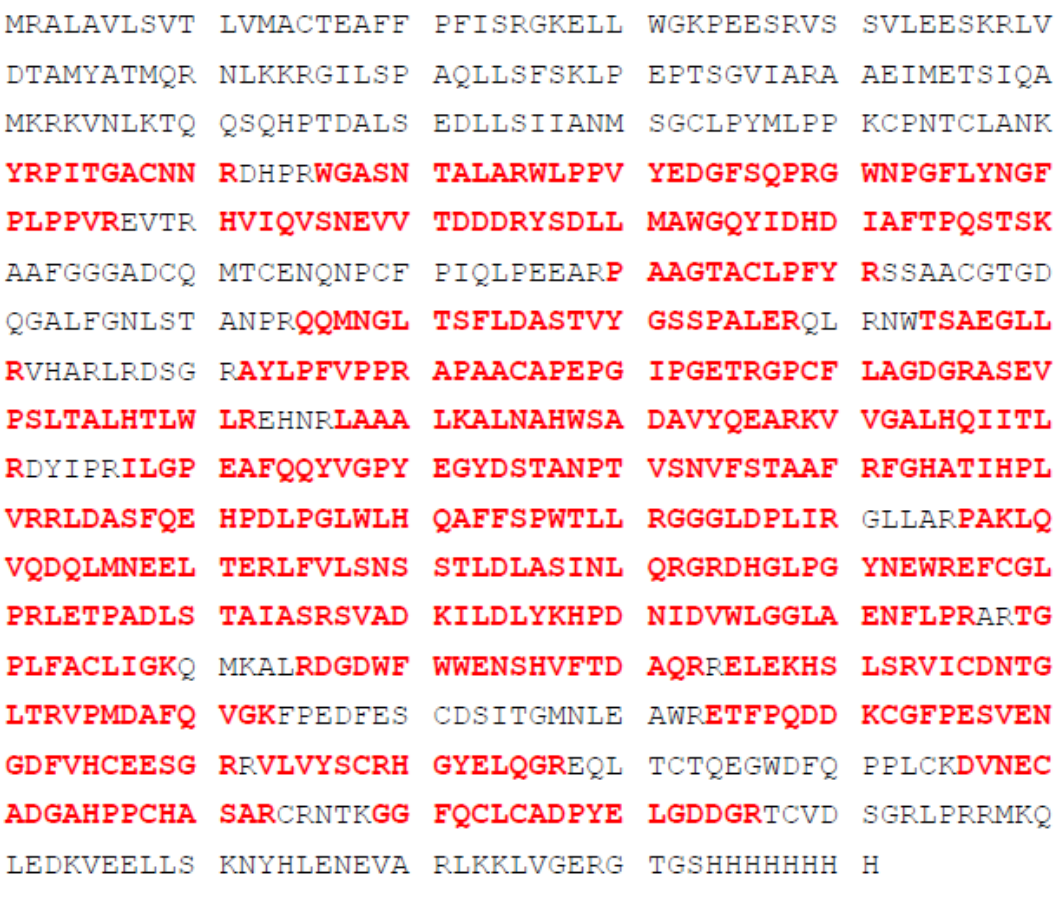

Figure S2 – Mass spectrometry analysis of ΔproTPOe-GCN4. Sequence coverage was reported as 70% with a protein score of 19294, making ΔproTPOe-GCN4 the most abundant species in the sample. Full length TPOe-GCN4 is in black lettering, with detected peptides highlighted in red. Note that residues 1 through 108 comprise the signal peptide and propeptide that are not incorporated into full length ΔproTPOe-GCN4, though are included here to demonstrate their successful non-inclusion in our construct.

30

```
  1 MRALAVLSVT LVMACTEAFF PFISRGKELL WGKPEESRVS SVLEESKRLV
 51 DTAMYATMQR NLKKRGILSP AQLLSFSKLP EPTSGVIARA AEIMETSIQA
101 MKRKVNLKTQ QSQHPTDALS EDLLSIIANM SGCLPYMLPP KCPNTCLANK
151 YRPITGACNN RDHPRWGASN TALARWLPPV YEDGFSQPRG WNPGFLYNGF
201 PLPPVREVTR HVIQVSNEVV TDDDRYSDLL MAWGQYIDHD IAFTPQSTSK
251 AAFGGGADCQ MTCENQNPCF PIQLPEEARP AAGTACLPFY RSSAACGTGD
301 QGALFGNLST ANPRQQMNGL TSFLDASTVY GSSPALERQL RNWTSAEGLL
351 RVHARLRDSG RAYLPFVPPR APAACAPEPG IPGETRGPCF LAGDGRASEV
401 PSLTALHTLW LREHNRLAAA LKALNAHWSA DAVYQEARKV VGALHQIITL
451 RDYIPRILGP EAFQQYVGPY EGYDSTANPT VSNVFSTAAF RFGHATIHPL
501 VRRLDASFQE HPDLPGLWLH QAFFSPWTLL RGGGLDPLIR GLLARPAKLQ
551 VQDQLMNEEL TERLFVLSNS STLDLASINL QRGRDHGLPG YNEWREFCGL
601 PRLETPADLS TAIASRSVAD KILDLYKHPD NIDVWLGGLA ENFLPRARTG
651 PLFACLIGKQ MKALRDGDWF WWENSHVFTD AQRRELEKHS LSRVICDNTG
701 LTRVPMDAFQ VGKFPEDFES CDSITGMNLE AWRETFPQDD KCGFPESVEN
751 GDFVHCEESG RRVLVYSCRH GYELQGREQL TCTQEGWDFQ PPLCKDVNEC
801 ADGAHPPCHA SARCRNTKGG FQCLCADPYE LGDDGRTCVD SGRLPRRMKQ
851 LEDKVEELLS KNYHLENEVA RLKKLVGERG TGSHHHHHHH H
```

31

32 **Figure S3 – Mass spectrometry analysis of suspected degraded ΔproTPOe-GCN4**
33 **fragment**. Sequence coverage was reported as 63% with a protein score of 8710, making
34 a degraded form of ΔproTPOe-GCN4 the most abundant species in the sample. Full
35 length ΔproTPOe-GCN4 is in black lettering, with detected peptides highlighted in red.
36 Note that residues 1 through 108 comprise the signal peptide and propeptide that are
37 not incorporated into full length ΔproTPOe-GCN4, though are included here to
38 demonstrate their successful non-inclusion in our construct.

39

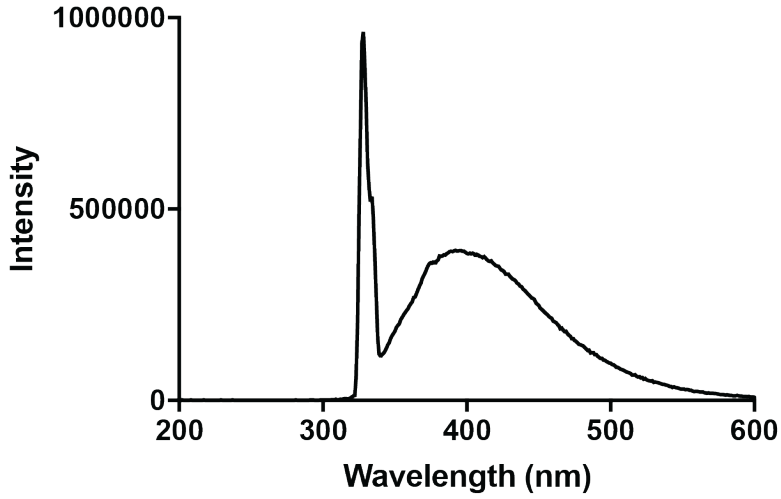

Figure S4 – Characterisation of enzyme activity of ΔproTPOe-GCN4. Spectral scan of ΔproTPOe-GCN4 after excitation using a wavelength of 330nm resulted in a Soret peak at 385nm, which is characteristic of hemoproteins. This indicates successful heme group incorporation into ΔproTPOe-GCN4.

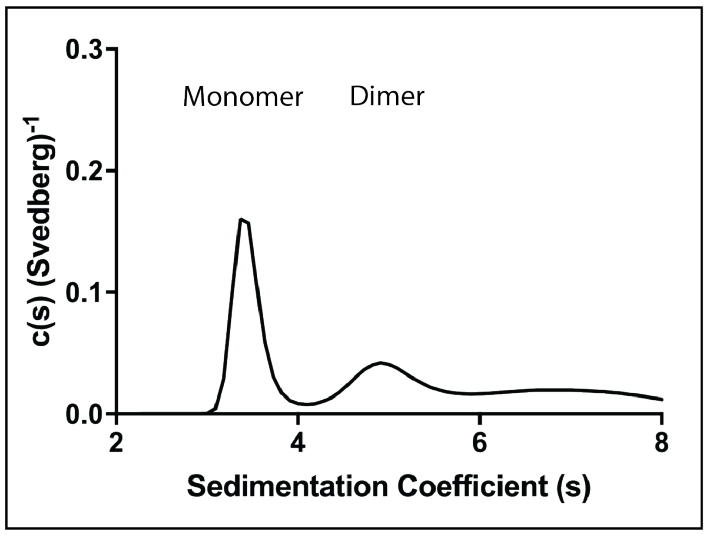

Figure S5 – Sedimentation distribution of ΔproTPOe-GCN4 alone. Two distinct species are detected at a $sw_{(20,w)}$ of 3.6 and 5.2 respectively. The molecular weights reported by c(M) analysis (not shown) in each case was 114 kDa and 201 kDa respectively, with a frictional ratio of 2.36. These molecular weights are consistent with a monomer (~110

kDa) and a dimer (~220 kDa) species. The relative abundance of each of the two species was analysed by SEDFIT (using area under the curve), with a monomer:dimer ratio of approximately 1.33:1, indicating the monomer is more abundant. The Stokes radii (Table S3) and frictional ratio of 2.36 suggest a non-spherical, elongated shape, consistent with our previous modelling (a frictional ratio of 1 would suggest a perfect sphere) (8).

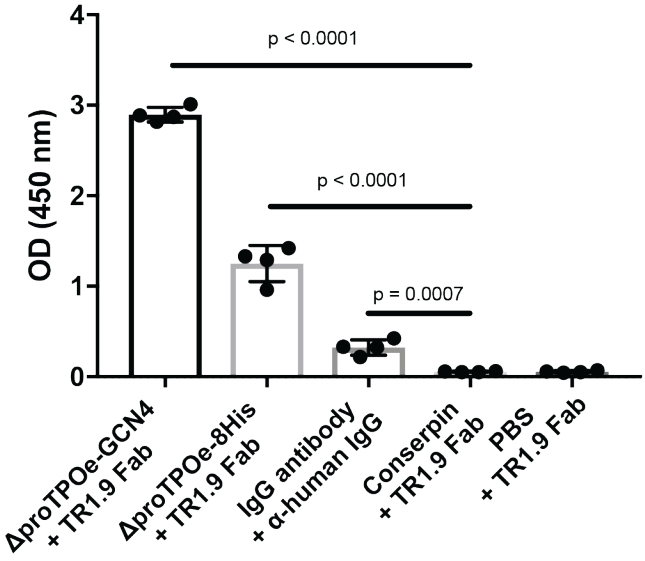

Figure S6 – ELISA results of TPO-Fab binding. TR1.9 Fab shows statistically significant binding to both TPO constructs, with a p value less than 0.0001 compared to a non-specific protein that does not have the required epitope (conserpin (20), negative control), as well as a PBS blank. IgG antibody and anti-human IgG was used as a positive control. Error bars are standard deviation from the mean and statistical tests were performed with a two-tailed t-test with a 95% confidence interval. All samples were performed in quadruplicate.

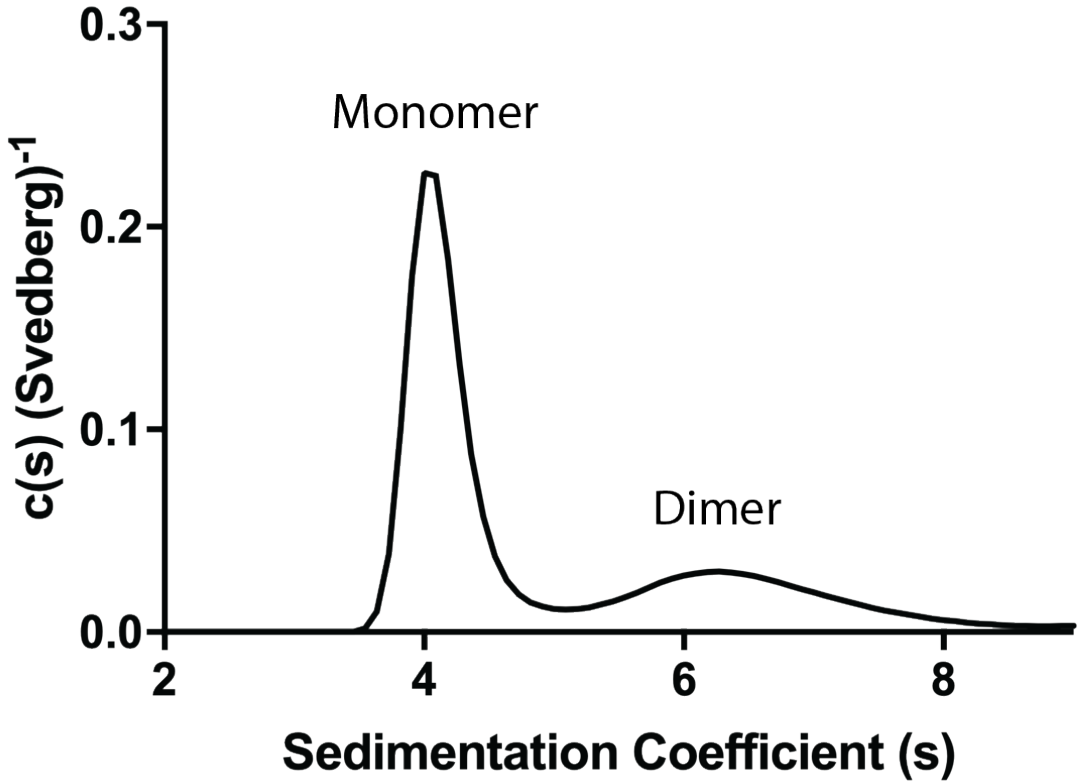

Figure S7 – Sedimentation distribution of ΔproTPOe-GCN4 bound to TR1.9 Fab. Two distinct species are detected at a $sw_{(20,w)}$ of 4.1 and 6.6 respectively. AUC analysis of an equimolar mixture of TR1.9 Fab and ΔproTPOe-GCN4 shows two peaks. The lack of a peak at 2.6S suggests that none, or very little of the Fab, remained un-complexed. Therefore, the two remaining peaks are most likely the TPO monomer/dimer peaks as observed for ΔproTPOe-8His (Fig. 5C). The observed shift in their standardised weight-average sedimentation coefficients (4.1S, 6.6S, respectively) suggest a change in their shape and mass, indicating Fab binding to both monomer and dimer ΔproTPOe-GCN4. The frictional ratio has also changed to 1.77 (from 2.36 with ΔproTPOe-GCN4 alone), indicating that TPO has taken a more spherical shape upon TR1.9 Fab binding. Importantly, the ratio of monomer and dimer has shifted to approximately 2:1.

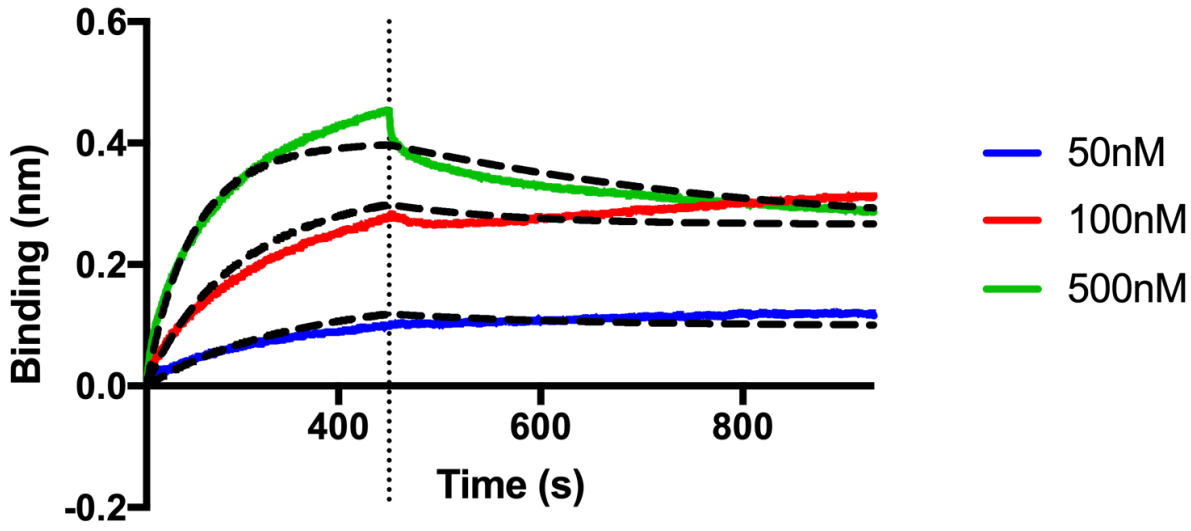

Figure S8 – Bio-layer interferometry (BLI) sensorgram data of ΔproTPOe-8His binding to Fab. Sensorgram curves according to a TR1.9 Fab concentration range of between 0 and 500 nM. ΔproTPOe-8His is immobilised on the biosensor surface. The data has been normalised against a blank run of buffer (1x PBS, pH 7.4). Vertical line at 450 s represents the end of the association phase. Dotted lines in black represent the fit calculated using a 1:1 binding model with global fitting within the BLItz Pro software. R^2 values for the calculated fit were reported as 0.97. K_D was calculated as 20 nM.

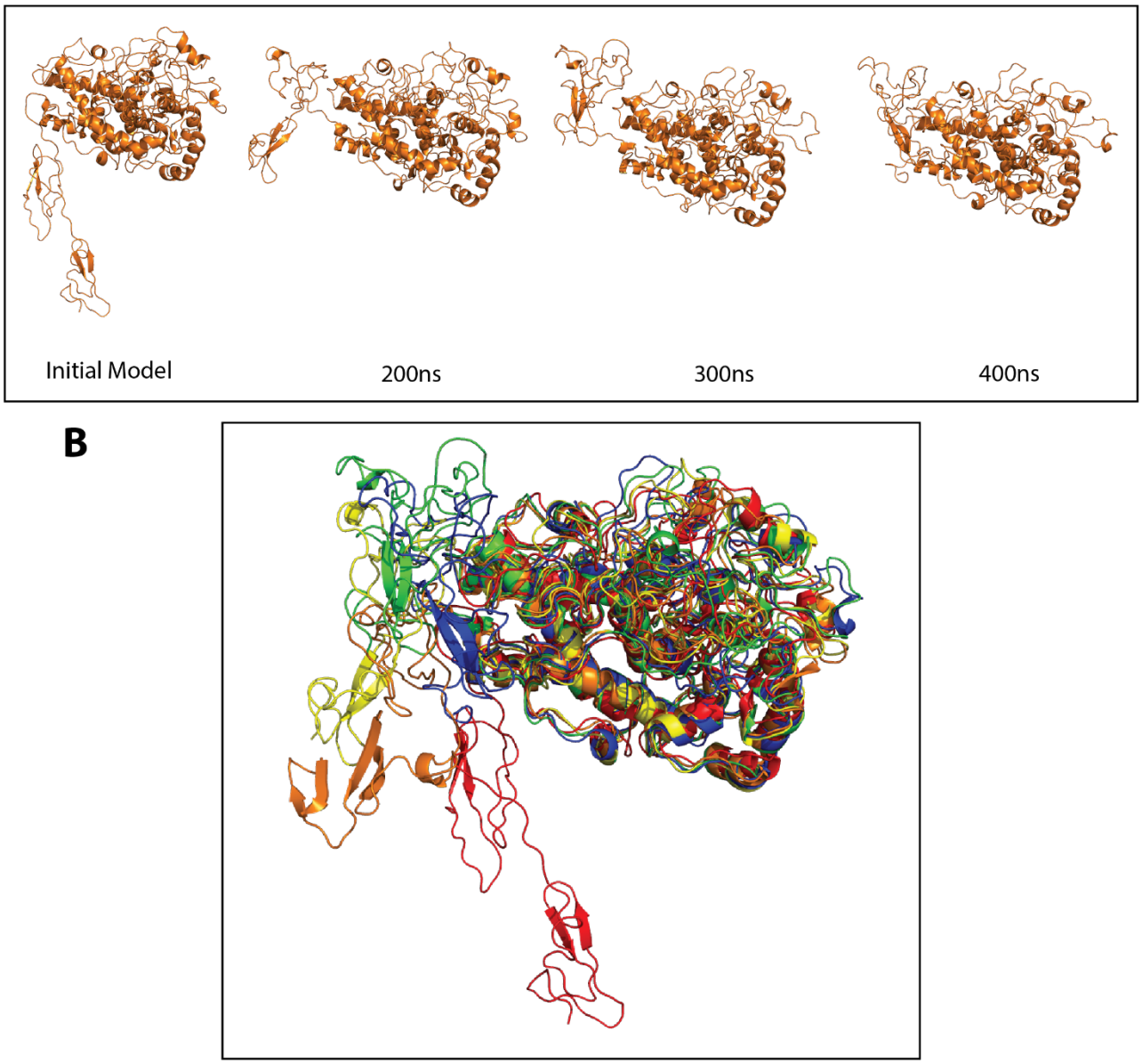

Figure S9 – Snapshots from the trans ΔproTPOe MD trajectory show TPO changing conformation from extended to more compact structure. Snapshots from the trans ΔproTPOe MD trajectory as presented in Figure 6. **(A)** Representation of the starting model from Le and co-workers (1), as well as *trans* ΔproTPOe after 200, 300 and 400 ns of simulation. **(B)** Structural superpositions of the above snapshots with the starting trans ΔproTPOe model in red. Orange indicates *trans* ΔproTPOe after 100 ns of simulation, yellow after 200 ns, green after 300 ns and blue after 400 ns.

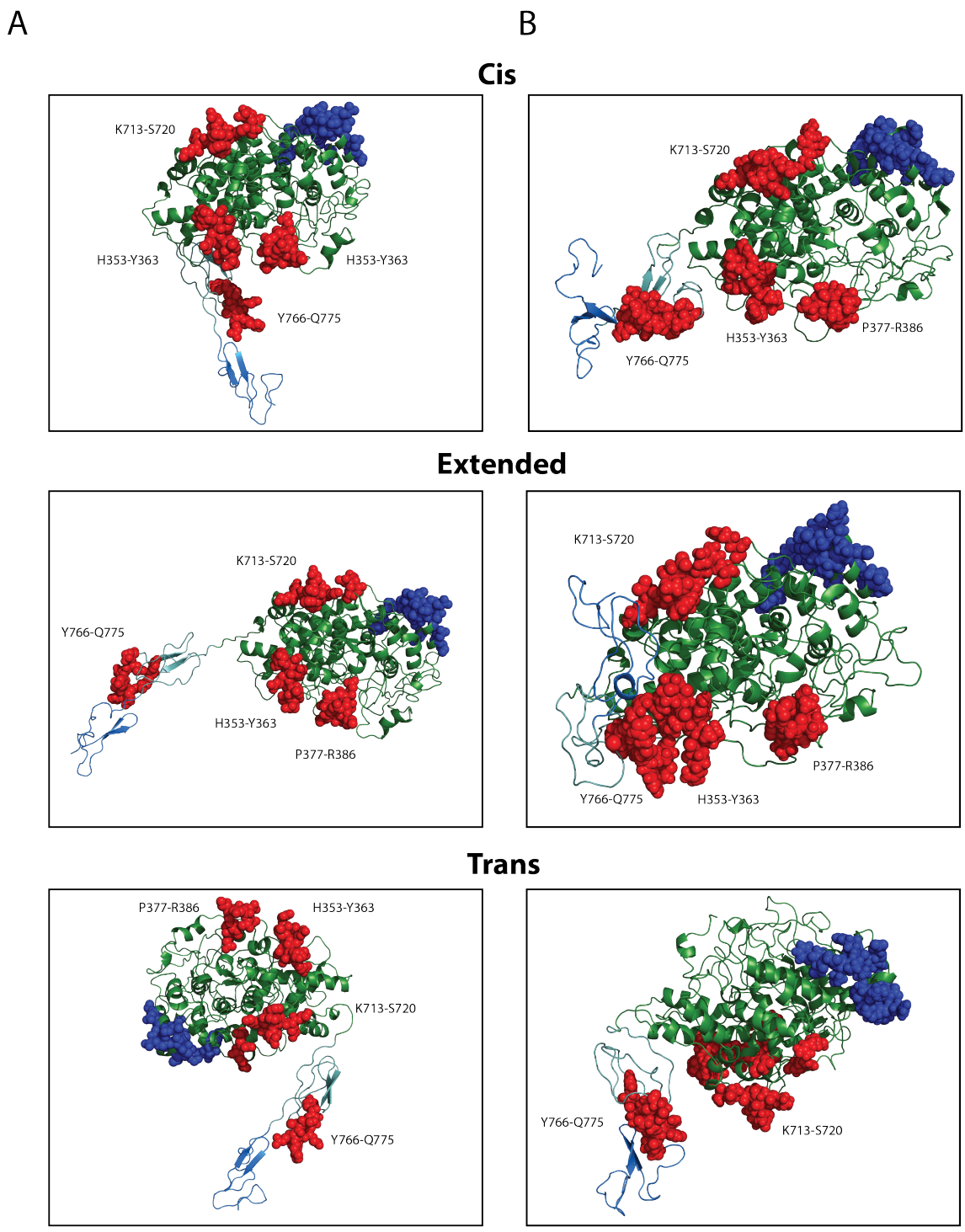

Figure S10 – IDRs in context of the MD simulations with starting structures. (A) TPO models (simulation starting structures) with IDRs highlighted. (**B)** Representative structures taken from the MD simulations for each of the *trans*, *cis* and *extended* forms of the ΔproTPOe monomer, as in Figure 7. IDR-A residues are highlighted by red spheres, and IDR-B residues by blue spheres.

The MPO-like domain, CCP-like domain and EGF-like domain are coloured in forest green, light teal and marine blue respectively (as in Figure 1).

Table S1 – Published residues involved in IDRs of TPO

Antibody Involved	Number of Reported Epitopes	Epitopes	Study
IDR-A			
T13	4	H353-Y363, P377-R386, K713-S720, Y766-Q775	(2-6)
ICA1	1	H353-Y363	(2,3)
TR1.9	2	K713, K713-S720	(2,4,7)
126TO10	3	R225, R646, D707	(8,9)
126TP1	3	R225, R646, D707	(8,9)
126TP7	1	R225	(9)
IDR-B			
126TP5	5	D620, D624, K627, D630, F597-E604	(8-10)
126TP14	5	D620, D624, K627, D630, F597-E604	(8-10)
131TP7	1	K627	(9)
SP1.4	1	F597-E604	(10)
TR1.8	1	T611-V618	(10)
WR1.7	1	F597-E604	(10)

The epitopes that have been identified as making up the immunodominant regions (IDRs) of TPO, named IDR-A and IDR-B.

Table S2 – Melting point data of ΔproTPOe-8His in different buffer conditions

Buffer	**pH**	**T_m** (°C)
50 mM HEPES, 250 mM NaCl	8.0	52.3
50 mM HEPES, 250 mM NaCl	7.0	55.2
50 mM Sodium Phosphate, 250 mM NaCl	6.0	54.7
50 mM Sodium Acetate, 250 mM NaCl	5.5	53.9
50 mM Glycine, 250 mM NaCl	4.0	53.6

Table S3 – Theoretical and calculated Stokes Radii (R_s) of TPO

Reference Dataset	**Equation**	**Stokes Radius (Å)**	
		Monomer	**Dimer**
Globular Folded Proteins	$R_s = (4.75)N^{0.29}$	32.52	39.75
Denatured Unfolded Proteins	$R_s = (2.21)N^{0.57}$	96.93	143.89
Analytical SEC of TPO with no TM domain		51.31	
AUC of ΔproTPOe-GCN4		75.7	91.4
AUC of ΔproTPOe-8His		64.9	77.1
AUC of ΔproTPOe-GCN4 with TR1.9		52.7	66.4
AUC of ΔproTPOe-8His with TR1.9		57.4	N/A

AUC, analytical ultracentrifugation; SEC, size exclusion chromatography; TM, transmembrane domain.

Table S4 – Model Fit Percentages

Model	Percentage of Molecules within the EM Map
Trans Monomer	73
Cis Monomer	72
Trans Dimer	54
Cis Dimer	59
Trans Monomer with Fab	53
Cis Monomer with Fab	55
Curled Monomer with Fab	58
Curled Monomer with scFv format of TR1.9	73
Trans Monomer with Fab sequentially fit*	68
Cis Monomer with Fab sequentially fit*	70
Trans Dimer with Fab	33
Cis Dimer with Fab	37

Fit percentages of various TPO models within the electron microscopy (EM) map. Asterisks (*) indicates configurations where TR 1.9 Fab was fitted into the available space in the envelope without regard to its epitope's location, rather than in a realistic orientation in which the complementarity determining regions (CDR) face the published epitope of K713-S720.

References

1. Le SN, Porebski BT, McCoey J, Fodor J, Riley B, Godlewska M, Gora M, Czarnocka B, Banga JP, Hoke DE, Kass I, Buckle AM. Modelling of Thyroid Peroxidase Reveals Insights into Its Enzyme Function and Autoantigenicity. *PloS one*. 2015;10(12):e0142615.
2. Bresson D, Cerutti M, Devauchelle G, Pugniere M, Roquet F, Bes C, Bossard C, Chardes T, Peraldi-Roux S. Localization of the discontinuous immunodominant region recognized by human anti-thyroperoxidase autoantibodies in autoimmune thyroid diseases. *The Journal of biological chemistry*. 2003;278(11):9560-9569.
3. Rebuffat SA, Bresson D, Nguyen B, Peraldi-Roux S. The key residues in the immunodominant region 353-363 of human thyroid peroxidase were identified. *International immunology*. 2006;18(7):1091-1099.
4. Bresson D, Pugniere M, Roquet F, Rebuffat SA, B NG, Cerutti M, Guo J, McLachlan SM, Rapoport B, Estienne V, Ruf J, Chardes T, Peraldi-Roux S. Directed mutagenesis in region 713-720 of human thyroperoxidase assigns 713KFPED717 residues as being involved in the B domain of the discontinuous immunodominant region recognized by human autoantibodies. *The Journal of biological chemistry*. 2004;279(37):39058-39067.
5. Williams DE, Le SN, Godlewska M, Hoke DE, Buckle AM. Thyroid Peroxidase as an Autoantigen in Hashimoto's Disease: Structure, Function, and Antigenicity. *Hormone and metabolic research = Hormon- und Stoffwechselforschung = Hormones et metabolisme*. 2018;50(12):908-921.
6. Estienne V, Duthoit C, Blanchin S, Montserret R, Durand-Gorde JM, Chartier M, Baty D, Carayon P, Ruf J. Analysis of a conformational B cell epitope of human thyroid peroxidase: identification of a tyrosine residue at a strategic location for immunodominance. *International immunology*. 2002;14(4):359-366.
7. Guo J, Yan XM, McLachlan SM, Rapoport B. Search for the autoantibody immunodominant region on thyroid peroxidase: epitopic footprinting with a human monoclonal autoantibody locates a facet on the native antigen containing a highly conformational epitope. *Journal of immunology (Baltimore, Md : 1950)*. 2001;166(2):1327-1333.
8. Dubska M, Banga JP, Plochocka D, Hoser G, Kemp EH, Sutton BJ, Gardas A, Gora M. Structural insights into autoreactive determinants in thyroid peroxidase composed of discontinuous and multiple key contact amino acid residues contributing to epitopes recognized by patients' autoantibodies. *Endocrinology*. 2006;147(12):5995-6003.
9. Gora M, Gardas A, Watson PF, Hobby P, Weetman AP, Sutton BJ, Banga JP. Key residues contributing to dominant conformational autoantigenic epitopes on thyroid peroxidase identified by mutagenesis. *Biochemical and biophysical research communications*. 2004;320(3):795-801.
10. Bresson D, Rebuffat SA, Nguyen B, Banga JP, Gardas A, Peraldi-Roux S. New Insights into the Conformational Dominant Epitopes on Thyroid Peroxidase Recognized by Human Autoantibodies. *Endocrinology*. 2005;146(6):2834-2844.